

Multiple Quantum Phase Transitions of Plutonium compounds

Munehisa Matsumoto¹, Quan Yin^{1,2}, Junya Otsuki³, Sergey Yu. Savrasov¹

¹*Department of Physics, University of California, Davis, California 95616, USA*

²*Department of Physics & Astronomy, Rutgers University, Piscataway, New Jersey 08854, USA,*

³*Department of Physics, Tohoku University, Sendai 980-8578, Japan*

(Dated: February 16, 2022)

We show by quantum Monte Carlo simulations of realistic Kondo lattice models derived from electronic-structure calculations that multiple quantum critical points can be realized in Plutonium-based materials. We place representative systems including PuCoGa₅ on a realistic Doniach phase diagram and identify the regions where the magnetically mediated superconductivity could occur. Solution of an inverse problem to restore the quasiparticle renormalization factor for f -electrons is shown to be sufficiently good to predict the trends among Sommerfeld coefficients and magnetism. Suggestion on the possible experimental verification for this scenario is given for PuAs.

PACS numbers: 71.27.+a, 75.30.Kz, 75.40.Mg

Motivation Discovery of unconventional superconductivity in PuCoGa₅ [1, 2] opened a new arena for the studies of strongly-correlated materials. It has the highest superconducting transition temperature $T_c = 18.5$ [K] among f -electron-based materials and it has been discussed to reside somewhere in between the Cerium-based heavy fermion (HF) superconductors and high- T_c cuprates, where the latter still challenges theoretical control from first-principles.

In the present work we make predictions on the magnetism and HF behavior of several Pu compounds including Pu-115's where the mechanism of possible magnetically-mediated superconductivity is discussed to be more complicated than their Cerium counterparts [3]. Furthermore, with experimental challenges such as the self-heating of samples due to the radiative nature of Pu nuclei, a computational guide should be of help regarding the determination of the linear coefficient of electronic heat capacity, so-called Sommerfeld coefficient γ . Our computational method is based on a recently-developed scheme for realistic Kondo lattice simulations [4, 5] which enabled us to predict the location of magnetic quantum critical point (QCP) [6] from electronic structure calculations [7] for HF materials.

Our main results are shown in Fig. 1 in the format of Doniach phase diagram [8] plotted with realistic settings for the target materials. Striking double-dome structure is seen both in the magnetic Doniach phase diagram of PuCoGa₅ plotted on (J_K, T_N) -plane and an analogous plot on (J_K, γ) -plane, where J_K is the Kondo coupling and T_N is the Neel temperature. For Pu-115's there are at least two antiferromagnetic phases with at least three QCP's. We see that Pu-115's are indeed separated from the first i.e. lowest-energy magnetic QCP, being consistent with the situation discussed in Ref. [3]. However we find that the second and third QCP's are encountered on J_K -axis and the realistic point for Pu-115 is actually in the proximity to the latter.

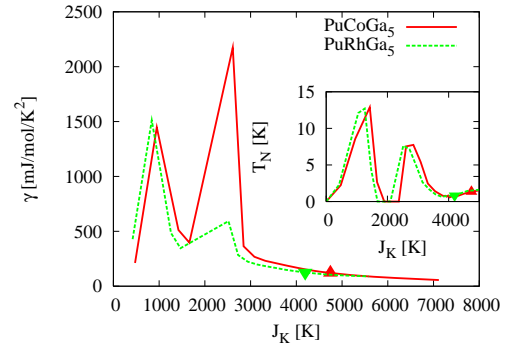


FIG. 1: (Color online) Summary of our results for Pu-115's on realistic Doniach phase diagram. The realistic data point is indicated by the symbol on the line for each target material. The main panel show the trend among Sommerfeld coefficients and the inset show the Néel temperatures.

Methods The electronic structure calculation based on local density approximation (LDA) combined with dynamical mean-field theory (DMFT) (LDA+DMFT) has been successful in addressing interesting properties of strongly-correlated materials [7]. What motivates us for the Kondo-lattice model (KLM) description of HF materials is that efficient and exact quantum Monte Carlo (QMC) simulations in low-temperature region are possible [9], typically around $O(10)$ [K] and down to $O(1)$ [K]. This advantage is due to having only f -spins and eliminating the f -electron charge degrees of freedom via Schrieffer-Wolff transformation [10] implemented in a realistic way [4]. This is in contrast to the fact that the standard LDA+DMFT based on solving the Anderson model, which was used e.g. in Ref. [11] for δ -Pu, typically can reach the temperatures down to $O(100)$ [K] if the core impurity problem is to be exactly solved by QMC method. Here, some basis-cutoff schemes have been implemented [12] to reduce the computational cost.

One of the reasons Plutonium compounds have been interesting and difficult to address is that they reside on

material	$N^{\text{tot}}(0)$	$N^f(0)$	$-\text{Tr}\Im\Delta(0)/\pi$ [eV]
PuCoGa ₅	34.33...	1.203...	0.705
PuRhGa ₅	33.03...	1.494...	0.912
δ -Pu	20.40...	2.781...	1.13
PuSe	17.30...	4.342...	0.619
PuTe	13.45...	0.7729...	0.360
PuAs	8.351...	0.6068...	0.255
PuSb	10.01...	0.2699...	0.193
PuBi	7.723...	0.2534...	0.133

TABLE I: Summary of LDA+Hubbard-I results for target materials. The unit of density of states, $N^{\text{tot}}(0)$ for all electrons and $N^f(0)$ for f -electrons on the Fermi level, is [states/Ry/cell].

the border of itinerancy and localization of $5f$ -electrons among actinides [13, 14]. At least for Pu-chalcogenides and pnictides, experimental evidence for localized $5f$ -electrons was revealed [15] and a recent theoretical work [16] agrees with that so these can be benchmark cases for the realistic KLM simulations. For Pu-115's it has been known that the Curie law persists down to the superconducting temperature for PuCoGa₅ [1] which supports the presence of localized $5f$ -electrons, but some attention must be reserved for a possible sample dependence: radiative Pu decays into U, which can introduce magnetic impurities. It is thus controversial whether the Curie-Weiss law is intrinsic or not [17]. Analyses of experiments point to $n_f = 5.03$ for δ -Pu [13] which we believe is sufficient for the KLM to work. The valence deduced from the calculations shows a much larger spread (between 4 [18] and 6 [19]) with the values of 5.2 for δ -Pu [20] and 5.26 for PuCoGa₅ [21] from most accurate CT-QMC calculations.

Our realistic KLM framework for the above-mentioned Pu compounds goes as follows. At the first stage LDA for s , p , and d -conduction electrons and Hubbard-I approximation [22] for the self-energy of localized f -electrons gives us the partial densities of states and hybridization functions as prescribed by LDA+DMFT framework [7]. The data are summarized in Table I. It is clear that Pu-115's have much higher energy scales than the Cerium ones [5]. At the second stage we solve the low-energy effective KLM Hamiltonian with dynamical-mean field theory [23, 24], utilizing state-of-the-art continuous-time quantum Monte Carlo (CT-QMC) impurity solver [9, 12, 25]. For the $5f$ -orbitals of Pu, it is known that there is a big spin-orbit splitting of 1 [eV] and the five possibly localized electrons fill in the lower $j = 5/2$ multiplet up to leaving one localized hole [26]. Photoemission experiments show that the level of the localized hole is separated from the Fermi level by 1 [eV] which is verified by our theoretical estimates. We neglect the crystal-field splittings which are known to be small in Pu compounds in the local $5f$ level.

Solving an inverse problem to restore f -electrons Even if we eliminated f -electrons and kept only f -spins in our KLM, part of the information for the localized f -electrons can be restored from the relation $\Sigma_c(i\omega_n) \equiv V^2/[i\omega_n - \epsilon_f - \Sigma_f(i\omega_n)]$, where Σ_c is our conduction-electron self energy, $i\omega_n = (2n+1)\pi T$ is the Matsubara frequency, $\epsilon_f = -1$ [eV] is the position of the impurity level, and Σ_f is the f -electron self-energy which we do not have explicitly in our KLM calculations. Provided that we reach the temperature for a given target material to be in a Fermi-liquid region concerning its f -electrons, which is mostly the case for Pu compounds, the quasiparticle renormalization factors are well defined and written as $z_x = (1 - \partial\Im\Sigma_x(i\omega_n)/\partial(i\omega_n))^{-1}$, with $x = c$ and f for conduction electrons and f -electrons, respectively. Here the derivative is taken at $i\omega_n = 0$. We get from the above definition of Σ_c the following inversion relation: $z_f = [|\Sigma_c(0)|^2/V^2]z_c/(1 - z_c)$. Because z 's are written in terms of the derivative of the corresponding self-energy at the lowest frequency, our effective low-energy description based on KLM enables a good solution of this inverse problem as far as z_f is concerned. The Sommerfeld coefficient $\gamma = (1/3)\pi^2 N_{\text{eff}}(0)$, where $N_{\text{eff}}(0)$ is the effective total density of states (DOS) on the Fermi level, can be estimated by $N_{\text{eff}}(0) = N_c(0)/z_c + N_f(0)/z_f$, where $N_c(0)$ is DOS of s , p , d -conduction electrons and $N_f(0)$ is that of localized f -electrons in our LDA+Hubbard-I calculations. With a given KLM, we extract z_c from Σ_c obtained after DMFT, invert it to z_f , and get the Sommerfeld coefficient γ with the above formula. In this way we can restore an analogue of Doniach phase diagram for γ as was shown in Fig. 1 for Pu-115's. The results on the realistic data point for each target material are summarized in Table II together with the experimental data taken from the literature. Our prediction follows the experimental trend among γ semi-quantitatively. We note that γ is sensitive to the estimate of the realistic point of J_K especially around QCP's, considering the sharp peak structure as seen in Fig. 1 for the plot of γ vs J_K . So the overall trend among materials is the most important result.

Magnetism and quasiparticle renormalizations The results for magnetism are schematically summarized in Fig. 2 for all target materials in the format of a rescaled Doniach phase diagram. It illustrates how we understand the results in the inset of Fig. 1 for Pu-115's. Striking multi-dome structure shows up together with multiple QCP's for materials with strong Kondo coupling. We find that Pu-115's are located in a region where antiferromagnetic long-range order is suppressed, possibly near a hidden or pseudo-QCP, within some numerical noise at the lowest reachable temperatures at present. Inspecting the distribution of materials around the QCP's in Fig. 2, we have pnictides on the left-hand side and chalcogenides on the right-hand side of the antiferromagnetic QCP. This is consistent with what has been known experimentally,

material	z_f	z_c	our γ	experimental γ
PuCoGa ₅	0.0403	0.0496	120	80 ^a -116 ^b
PuRhGa ₅	0.0367	0.0462	130	50 ^a -80 ^c
δ -Pu	0.0625	0.0738	49	50-64 ^d
PuSe	0.0480	0.0232	110	90 ^e
PuTe	0.00883	0.0313	85	30 ^f -60 ^e
PuAs	0.0588	0.00456	295	
PuSb	0.0231	0.0168	102	6 ^b -20 ^g
PuBi	0.00202	0.0965	35	

^a Ref. [30] ^b Ref. [31] ^c Ref. [32] ^d Ref. [33] ^e Ref. [29] ^f Ref. [34] ^g Ref. [35]

TABLE II: Summary of our data obtained with realistic Kondo lattice simulations and our prediction for γ based on them. The unit of γ is [mJ/mol/K²]. Experimentally known results are taken from the literature.

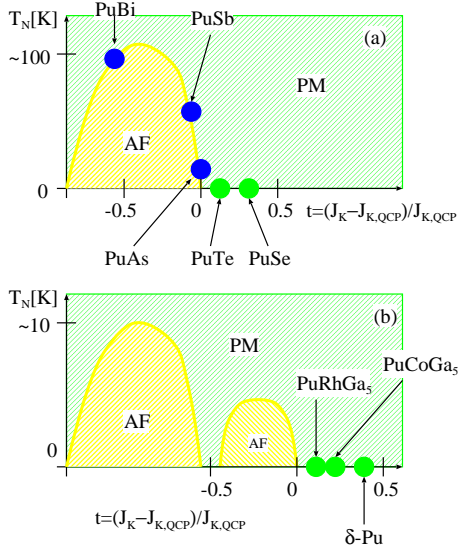


FIG. 2: (Color online) Schematic summary of our magnetic phase diagrams for Pu compounds plotted on the (t, T_N) -plane where $t \equiv (J_K - J_{K,QCP})/J_{K,QCP}$ is the rescaled Kondo coupling with $J_{K,QCP}$ being the first QCP in (a) and the third QCP in (b).

that is, pnictides such as PuAs, PuSb [27], and PuBi [28] are magnets and chalcogenides such as PuSe and PuTe are paramagnets [29]. The actual magnetism is strongly spatially anisotropic [14, 28] whose treatment is unfortunately beyond the level of single-site DMFT description. For now we will leave the issue of ordering wavevectors for future projects and focus on the trends across target materials spanning between magnetism and HF behavior. The characteristic energy scales of Kondo-screening and magnetic ordering have been captured by fully incorporating the frequency-dependence of the hybridization.

Multi-dome structure together with multiple QCP's shown in Fig. 1 for Pu-115's can be understood in terms of strong-coupling nature of the Kondo lattice [36] based

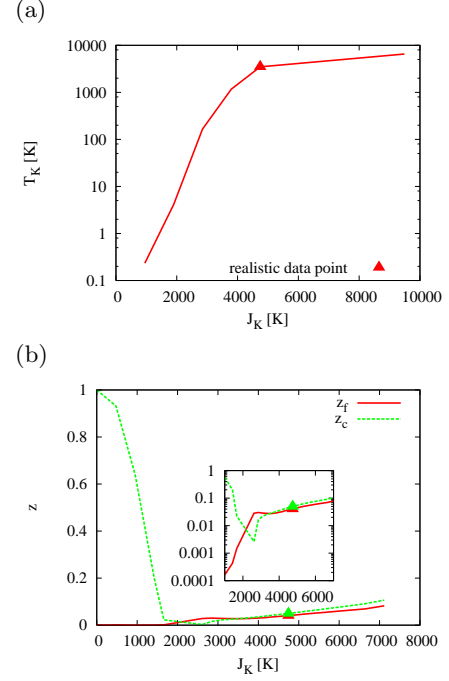


FIG. 3: (Color online) Analogue of Doniach phase diagram for (a) Kondo temperature and (b) quasiparticle renormalization factors for PuCoGa₅. The inset in (b) is a zoom-up picture around the first QCP with the vertical axis plotted in logarithm.

on the growth of characteristic Kondo energy scale T_K with respect to J_K as shown in Fig. 3 (a) which is obtained from our local susceptibility data. Simple perturbative arguments also prompt for two crossover points between $T_{RKKY} \sim J_K^2 \rho$ and $T_K \sim \exp[-1/(J_K \rho)]/\rho$ temperature scales, where the latter can saturate at some point with respect to large J_K while the former keeps on growing. Here ρ is the characteristic DOS.

We demonstrate our predictive power regarding T_K also for the case of δ -Pu where we get $T_K \sim 10^3$ [K] from our local susceptibility data which is seen to be close to the previous results, $T_K \sim 700$ [K] in Ref. [20]. We note that the Kondo screening energy scale is approaching a comparative scale to the characteristic bandwidth, or the kinetic energy of the conduction electrons which is $O(1)$ [eV]. Such situation had been discussed in the literature [36, 37] in the context of models, which is now found to be realized in Plutonium heavy-fermion materials.

The behavior of quasiparticle renormalization factors z_x ($x = c$ or f) as shown in Fig. 3 (b) further gives the physical picture: starting from $J_K = 0$ where there are free conduction electrons and completely localized f -electrons with $(z_c, z_f) = (1, 0)$, the former gradually gets renormalized toward the first QCP and f -electrons gets “delocalized” in the sense that they start to take part in Fermi surface (FS) [38, 39]. Passing the first QCP,

heavy quasiparticles composed both of conduction electrons and f -electrons evolve together after z_c has shown a dip around the first QCP, letting f -spins show up again with the underscreening effects that correspond to the slightly elevated z_c . Thus after the revival of magnetism the same thing can happen again and could repeat itself, with the re-defined much smaller energy scales every time, all the way to the $J_K \rightarrow \infty$ limit, being consistent with the phase diagram obtained in Ref. [36].

This strong-coupling KLM scenario for Pu compounds can in principle be checked by de Haas-van Alphen experiments which would measure the size of the FS to see if it counts the number of “localized” f -electrons. The ferromagnetic phase of PuAs should be the one with the “large” FS including the spins of localized $5f$ -electrons. This phase would be in contrast to the typical magnetic phases in HF compounds with the “small” FS, being located in the weak-coupling region. Following the method of Ref. [39], we can track the evolution of large FS for representative Pu compounds obtained from $-\Re\Sigma_c(i\omega_n)|_{i\omega_n=0}$ and we find that PuAs shows a remarkable evolution of “large” FS, which is to be compared with experiments to see if the strong-coupling KLM picture can hold.

Conclusions We have found that multiple QCP’s show up for Plutonium-based materials that have stronger Kondo couplings than their Cerium counterparts. Our methodology captures the quasiparticle renormalization factor and the characteristic energy scale correctly. The striking multi-dome feature of the Doniach phase diagrams for Pu-115’s and δ -Pu as well as the magnetic and HF behavior among Pu pnictides and chalcogenides is understood on the basis of strong-coupling limit of KLM. This picture can be verified by looking at the size of the Fermi surface for PuAs.

The authors thank E. D. Bauer, A. V. Chubukov, P. Coleman, N. J. Curro, R. Dong, M. J. Han, K. Haule, K. Kim, G. Kotliar, H. Shishido, Y.-F. Yang, C.-H. Yee for discussions. The present numerical calculations have been done on “Chinook” in Pacific Northwest National Laboratory. This work was supported by DOE NEUP Contract No. 00088708.

[1] J. L. Sarrao *et al.*, Nature **420**, 297 (2002).
 [2] N.J. Curro *et al.*, Nature **434**, 622 (2005).
 [3] R. Flint, M. Dzero, and P. Coleman, Nat. Phys. **4**, 643 (2008).
 [4] M. Matsumoto, M. J. Han, J. Otsuki, and S. Y. Savrasov, Phys. Rev. Lett. **103**, 096403 (2009).
 [5] M. Matsumoto, M. J. Han, J. Otsuki, and S. Y. Savrasov, Phys. Rev. B **82**, 180515(R) (2010).
 [6] For a review, see S. Sachdev, *Quantum Phase Transitions* (Cambridge Univ. Press, New York, 1999).
 [7] For a review, see G. Kotliar, S. Y. Savrasov, K. Haule,

V. S. Oudovenko, O. Parcollet, C. A. Marianetti, Rev. Mod. Phys. **78**, 865 (2006).
 [8] S. Doniach, Physica B **91**, 231 (1977).
 [9] J. Otsuki, H. Kusunose, P. Werner and Y. Kuramoto, J. Phys. Soc. Jpn. **76**, 114707 (2007).
 [10] J. R. Schrieffer and P. A. Wolff, Phys. Rev. **149**, 491 (1966).
 [11] C. A. Marianetti, K. Haule, G. Kotliar, and M. J. Fluss, Phys. Rev. Lett. **101**, 056403 (2008).
 [12] K. Haule, Phys. Rev. B **75**, 155113 (2007).
 [13] For a review, see K. T. Moore and G. van der Laan, Rev. Mod. Phys. **81**, 235 (2009).
 [14] For a review, see P. Santini, R. L  manski, and P. Erd  s, Adv. Phys. **48**, 537 (1999).
 [15] T. Gouder, F. Wastin, J. Rebizant, and L. Havela, Phys. Rev. Lett. **84**, 3378 (2000).
 [16] C. H. Yee, G. Kotliar, and K. Haule, Phys. Rev. B **81**, 035105 (2010).
 [17] A. Hiess *et al.*, Phys. Rev. Lett. **100**, 076403 (2008).
 [18] O. Eriksson, J. D. Becker, A. V. Balatsky, and J. M. Wills, J. Alloys. Compd. **287**, 1 (1999).
 [19] L. Havela *et al.*, J. Alloys. Compd **444-445**, 88 (2007).
 [20] J. H. Shim, K. Haule, and G. Kotliar, Nature **446**, 513 (2007).
 [21] M. E. Pezzoli, K. Haule, and G. Kotliar, Phys. Rev. Lett. **106**, 016403 (2011).
 [22] J. Hubbard. Proc. R. Soc. London, Ser. A **276**, 238 (1963); **277**, 237 (1964); **281**, 401 (1964).
 [23] A. Georges, G. Kotliar, W. Krauth, and M. J. Rozenberg, Rev. Mod. Phys. **68**, 13 (1996).
 [24] J. Otsuki, H. Kusunose, and Y. Kuramoto, J. Phys. Soc. Jpn. **78**, 014702 (2009).
 [25] P. Werner, A. Comanac, L. de’ Medici, M. Troyer, and A. J. Millis, Phys. Rev. Lett. **97**, 076405 (2006).
 [26] The analogy between Cerium and Plutonium compounds was discussed earlier in the following paper: B. R. Cooper, P. Thayamballi, J. C. Spirlet, W. M  ller, and O. Vogt, Phys. Rev. Lett. **51**, 2418 (1983). Also a similar modeling has been discussed in a recent paper: C. D. Batista, J. E. Gubernatis, T. Durakiewicz, and J. J. Joyce, Phys. Rev. Lett. **101**, 016403 (2008).
 [27] P. Burlet *et al.*, Phys. Rev. B **30**, 6660 (1984).
 [28] K. Mattenberger, O. Vogt, J. C. Spirlet, and J. Rebizant, J. Mag. Mag. Materials **54-57**, 539 (1986).
 [29] J. M. Fournier *et al.*, Physica B **163**, 493 (1990).
 [30] J. D. Thompson, N. J. Curro, T. Park, E. D. Bauer, and J. L. Sarrao, J. Alloys. Compounds **444-445**, 19 (2007).
 [31] P. Javorsk  y, F. Wastin, E. Colineau, J. Rebizant, P. Boulet, G. Stewart, Journal of Nuclear Materials **344**, 50 (2005).
 [32] J. L. Sarrao and J. D. Thompson, J. Phys. Soc. Jpn. **76**, 051013 (2007).
 [33] J. C. Lashley *et al.*, Phys. Rev. Lett. **91**, 205901 (2003).
 [34] G. R. Stewart, R. G. Haire, J. C. Spirlet, and J. Rebizant, J. Alloys. Compounds **177**, 167 (1991).
 [35] R. O. A. Hall, A. J. Jeffery, and M. J. Mortimer, J. Less-Common Metals, **121** 181 (1986).
 [36] C. Lacroix, Solid State Communications **54**, 991 (1985).
 [37] M. Sigrist, H. Tsunetsugu, K. Ueda, and T. M. Rice, Phys. Rev. B **46**, 13838 (1992).
 [38] R. M. Martin, Phys. Rev. Lett. **48**, 362 (1982).
 [39] J. Otsuki, H. Kusunose, and Y. Kuramoto, Phys. Rev. Lett. **102**, 017202 (2009).